Intramolecular Charge Transfer and Photochemical Isomerization in Donor/Acceptor-Substituted Butadienes

Riju Davis and Suresh Das*,†

Photochemistry Research Unit, Regional Research Laboratory, CSIR, Trivandrum 695019, India

Mathew George, Sergey Druzhinin, and Klaas A. Zachariasse*

Max-Planck-Institut für biophysikalische Chemie, Spektroskopie und Photochemische Kinetik, 37070 Göttingen, Germany

Received: November 17, 2000; In Final Form: February 26, 2001

Intramolecular charge transfers, triplet state properties, and photoisomerization of five donor/acceptor (D/A) substituted butadienes were investigated. Four of these derivatives (**1**−**4**) show dual fluorescence arising from a locally excited (LE) state and a considerably more polar intramolecular charge transfer (ICT) state. The presence of an amino substituent with the nitrogen atom directly attached to the butadiene chain is essential for observing dual fluorescence in this class of compounds. The compounds undergo *E*−*Z* photoisomerization from the excited singlet state with a quantum efficiency of about 0.1 in benzene at room temperature. The intersystem crossing efficiency for these compounds is negligible. The triplet excited-state properties of the five butadienes have been characterized via triplet−triplet sensitization with benzophenone as the donor.

Introduction

The synthesis and study of new organic molecules possessing second-order nonlinear optical (NLO) properties has been a subject of intense activity due to the potential applications of these molecules in integrated optics, such as optical modulation, optical switching, and optical data-processing.[1−8] The ability to optimize the NLO properties of organic materials relies on a fundamental understanding of the interrelationships between chemical structure and molecular nonlinearities.[1−4] Materials capable of second harmonic generation are associated with highly polarizable molecules, with large second-order molecular polarizability (β) values. Such molecules can be obtained by linking strong electron donor (D) and acceptor (A) groups through polarizable π-conjugated bridges. D/A molecules are usually characterized by large oscillator strengths for the ground to excited state transition, large dipole moment changes between the ground and excited state, and intramolecular charge transfer (ICT) transitions at relatively low energies. There has been a growing interest in the design of molecular systems in which the second-order nonlinear optical properties can be switched on and off using external light or electric stimuli.[9]

D/A-substituted butadienes are reported to have good NLO properties.[10,11] Intramolecular charge transfer has also been recently reported for nitro- and cyano-substituted 1,4-diphenylbutadienes.[12] We have earlier reported on the nonlinear optical properties of some donor−acceptor substituted butadienes containing L-prolinol as the donor.[11] One of these molecules shows an anomalous red-shifted fluorescence band in addition to the normal Stokes-shifted band. Several molecules in which ICT reactions take place show the phenomenon of dual luminescence. The origin of these processes is presently under debate.[13−18] To explore the mechanism of dual luminescence exhibited by the D/A-substituted butadienes, a series of such compounds containing different amino groups as donor substituents and 1,3-indanedione as the acceptor moiety (Chart 1) have been investigated. These molecules are also capable of undergoing photoisomerization, which makes them potentially useful for designing photoswitchable NLO materials. Photoisomerization in linear polyenes is also of interest in view of the related processes that occur in retinal polyenes.[19−21] Here, we report on the detailed study of the intramolecular charge transfer process as well as photoisomerization from the excited singlet and triplet states of this class of D/A-substituted butadienes.

CHART 1

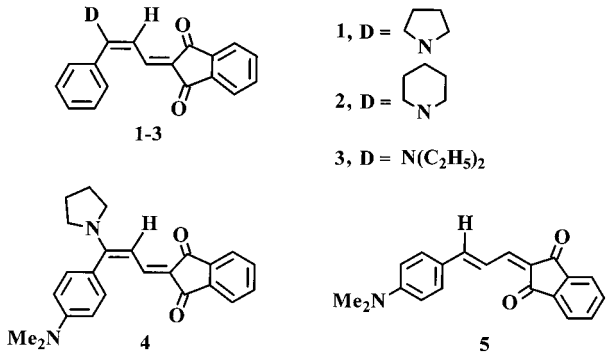

Experimental Section

Materials. The D/A-substituted butadienes, **1**−**4**, were synthesized using methods reported earlier.[11] Substance **5** was synthesized by the condensation of *N*,*N*-dimethylaminocinnamaldehyde with 1,3-indanedione. The compounds were purified by column chromatography followed by repeated recrystallization from 1:9 methanol/chloroform (**1**), benzene (**2**, **3**, and **4**) and 4:1 ethyl acetate/*n*-hexane (**5**). The structures of the butadiene derivatives, **1**−**5**, (Chart 1) were confirmed by NMR, IR, and high-resolution mass spectral (HRMS) analysis.[22]

† Email: sdaas@rediffmail.com.

10.1021/jp004245+ CCC: $20.00
Published on Web 04/20/2001

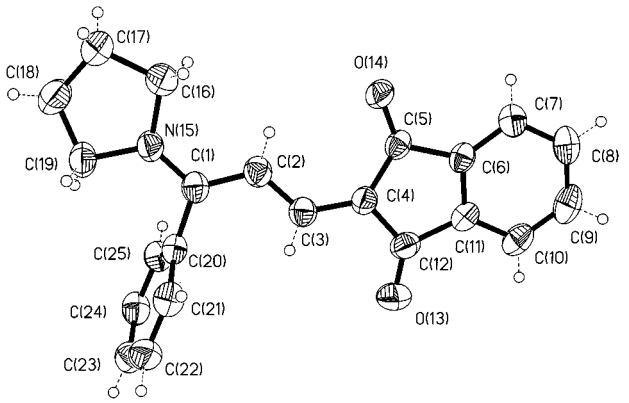

Figure 1. Molecular structure of **1** obtained from the X-ray crystallographic analysis, see text.

The purity of these compounds (>99%) was confirmed by high-pressure liquid chromatography. Spectroscopic grade solvents were used for all the spectroscopic studies. Solvents were purified by chromatography over alumina. Toluene and benzene were refluxed with sodium and distilled.

Optical Measurements. Absorption spectra were recorded on a Shimadzu UV-3101PC spectrophotometer. The excitation and emission spectra were measured on a SPEX Fluorolog F112X spectrofluorimeter. Fluorescence quantum yields, with an estimated reproducibility of around 10%, were determined by comparison with Rhodamine 6G in ethanol ($\Phi_{flu} = 0.9$), which was used as the fluorescence standard. Solutions with the same optical density at the excitation wavelength were used.

The fluorescence decay times were determined with a picosecond laser setup (excitation wavelength λ_{exc}, 413 nm).[17,23] The instrument response function has a half-width of 20−35 ps, and the reproducibility of the measured decay times is better than 2% for the longer times, but for the shorter decay times around 5 ps, the estimated accuracy will be 10%. The analysis procedure of fluorescence decays was carried out as described previously.[17,23]

Nanosecond laser flash photolysis experiments were carried out at room temperature on an Applied Photophysics model LKS-20 laser kinetic spectrometer with the third harmonic (355 nm) of a Quanta Ray GCR-12 Nd:YAG laser with a pulse duration of 10 ns and energy of 70 mJ/pulse. All solutions were degassed by bubbling argon for a minimum of 15 min.

A 200 W high-pressure mercury lamp, in combination with an Oriel grating monochromator (model 77250), was used as the light source for steady-state photolysis experiments. For estimating the steady-state quantum yield of photoisomerization, the intensity of the light (I) absorbed by substrate was determined by using the Reinecke's salt actinometry.[24] The light intensity (I_0) transmitted through the solvent was first measured using the actinometer solution in a cuvette (1 cm) placed behind a cuvette containing the pure solvent. The solvent was replaced with a solution containing the substrate and a fresh solution of the actinometer was used to estimate the light intensity (I_1) transmitted through the solution. The light intensity (I) absorbed by the substrate is equal to the difference (I_0-I_1) between these light intensities.

Results and Discussion

Molecular Structure. The molecular structure of **1** was determined by X-ray crystal analysis,[25] for which good quality crystals could be obtained from a 1:9 solvent mixture of methanol and chloroform. The molecular geometry of **1** with the atomic labeling is shown in Figure 1. The figure shows the *E* isomer to be the preferred configuration. It is seen that the pyrrolidine and the indanedione moieties are largely coplanar, with the dihedral angles N(15)C(1)C(2)C(3), C(1)C(2)C(3)C(4), and C(2)C(3)C(4)C(5) equal to 175.2°, 175.6°, and 1.8°, respectively. The phenyl group, on the other hand, is perpendicularly twisted out of this plane, with the dihedral angle C(2)-C(1)C(20)C(21) being equal to 85.2°. The C(1)−N(15) bond length is very short for a single bond (1.334 (3) Å), indicating that the pyrrolidino group is in strong conjugation with the indanedione moiety through the butadiene chain. This is also supported by the lack of bond length alternation in the buatadiene chain, for which the C(1)−C(2), C(2)−C(3), and C(3)−C(4) bonds are 1.396 (3), 1.387 (4), and 1.391 (3) Å, respectively.[4]

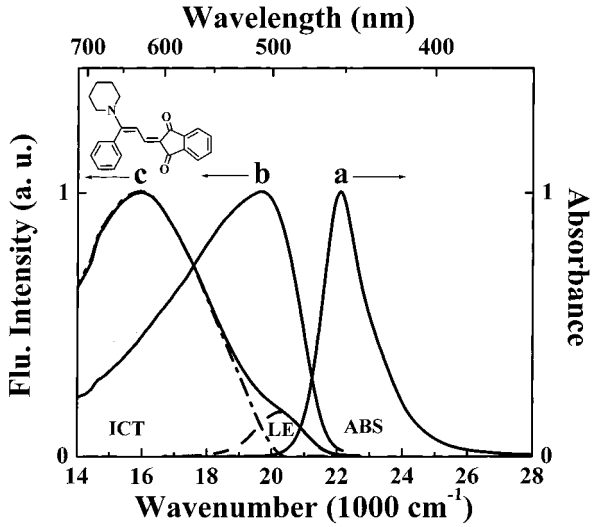

Figure 2. Normalized absorption and fluorescence spectra of **2** at 25 °C: (a) absorption spectrum in acetonitrile, (b) fluorescence spectrum in diisopropyl ether, and (c) fluorescence spectrum in acetonitrile.

Absorption and Fluorescence. The normalized absorption spectrum of **2** in acetonitrile as well as its fluorescence spectra in diisopropyl ether and acetonitrile at 25 °C are shown in Figure 2. The maximum of the absorption band is practically independent of solvent polarity (Table 1). Similar observations were made in the case of compounds **1**, **3**, and **4**, which can be attributed to a negligible change in dipole moment between the ground and the corresponding Franck−Condon (FC) excited state of these molecules. The absorption maximum of **5**, on the other hand, shows a bathochromic shift with increasing solvent polarity, indicating an increase in the dipole moment in the excited FC state for this compound. The absorption and fluorescence properties of the molecules studied are summarized in Table 1.

The compounds **1**−**4** have low fluorescence quantum yields between 3×10^{-3} and 10^{-4} (Table 1). Unlike the negligible effect of solvent polarity on their absorption spectra, the effect on their fluorescence spectra is quite significant. In a weakly polar solvent such as diisopropyl ether ($\epsilon = 3.88$ (25 °C)), the emission spectrum shows a maximum around 500 nm and a broad tail in the longer wavelength region (Figure 2, curve b). With increasing solvent polarity, there is a relative increase in intensity at longer wavelengths and in a highly polar solvent such as acetonitrile ($\epsilon = 37.5$ (25 °C)), an ICT fluorescence band with a smaller LE band at higher energies can be seen (Figure 2, curve c).

Dual fluorescence in molecules possessing ICT transitions can generally be described on the basis of the mechanism shown in Scheme 1.[15]

TABLE 1: Absorption and Emission Maxima in cm^{-1} and Fluorescence Quantum Yields Φ_{Flu} of 1−5 in Solvents of Different Polarity at 25 °C

	Toluene		Diisopropyl ether		Acetonitrile		DMSO		
compd	abs	em	abs	em	abs	em	abs	em	Φ_{flu}[a]
1	21 980	20 530	22 220	20 330, 17 210	22 220	20 700, 16 580	21 980	20 660, 16 290	0.0004
2	21 980	20 330	22 220	20 120, 17 450	22 220	20 200, 16 750	21 980	20 410, 16 560	0.0002
3	21 980	20 760	22 220	20 280, 17 000	22 220	20 750, 16 750	21 980	20 200, 16 420	0.0003
4	21 740	19 490	21 980	19 420	21 980	16 420	21 740	16 000	0.003
5	19 230	17 010	19 610	16 860	19 050	15 630	18 020	15 220	0.03

[a] In toluene.

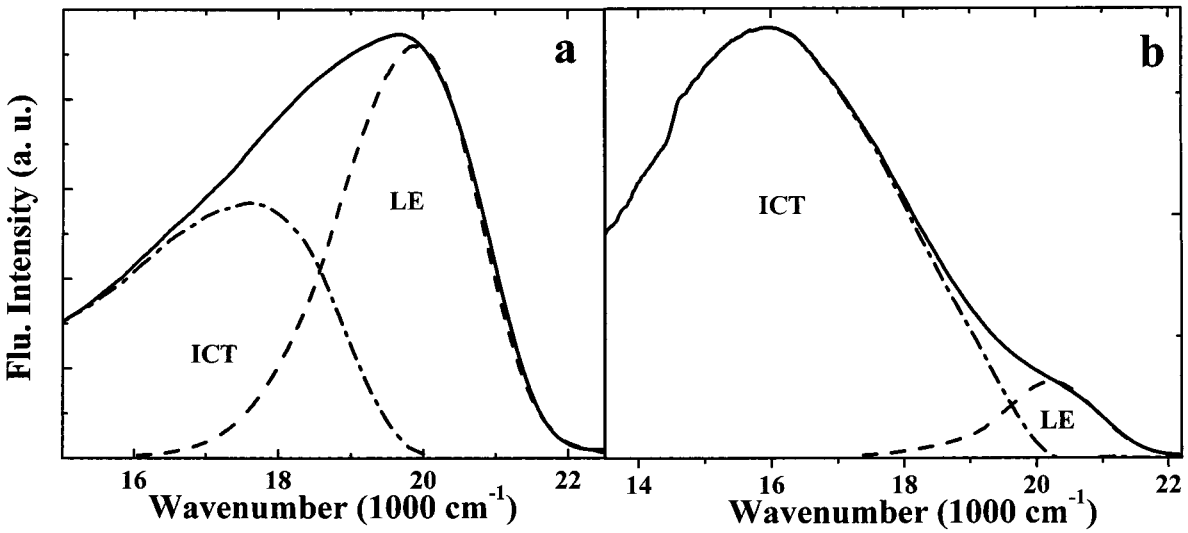

Figure 3. Fluorescence spectra of **2** at 25 °C in (a) diisopropyl ether and (b) acetonitrile. The separate emissions from the LE and ICT state are shown. The fluorescence spectrum of **5** in the corresponding solvent (approximately shifted) was adopted to represent the LE fluorescence band in the spectral subtraction procedure.

SCHEME 1

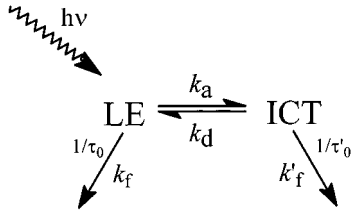

According to this mechanism, the dual emission arises from two states termed as locally excited (LE) and intramolecular charge transfer (ICT) states in equilibrium. The LE state refers to a state which can be reached directly by absorption from S_0. In the ICT excited state, which originates from the LE state, considerable charge separation between the donor and the acceptor groups is expected. The separated LE and ICT fluorescence bands of **2** in diisopropyl ether and acetonitrile are shown in Figure 3. Similarly, distinct LE and ICT bands were also observed for the compounds **1** and **3**.

The kinetics of the dual fluorescence can be treated on the basis of the mechanism shown in Scheme 1, where k_a and k_d are the rate constants of the forward and backward ICT reactions, τ_0(LE) and τ_0'(ICT) are the fluorescence lifetimes. The radiative rate constants, k_f(LE) and k'_f(ICT) have also been indicated. The forward and backward reactions represented by this scheme commonly involve an orientational relaxation of the solvent molecules following the changes in charge distribution.

Dipole Moments. Figure 4 shows the plot of the LE and ICT fluorescence band maxima of **2** against the solvent polarity parameter ($f - f'$)

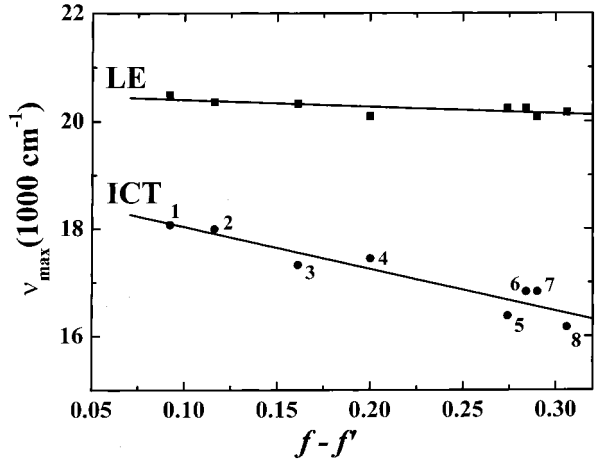

Figure 4. Solvatochromic plots of the emission maxima of the locally excited state (■) and the ICT state (●) of **2** at 25 °C versus the macroscopic solvent polarity parameter $f-f'$ (eq 3). Solvents: (1) di(*n*-butyl) ether, (2) di(*n*-propyl) ether, (3) diethyl ether, (4) ethyl acetate, (5) acetone, (6) dimethylformamide, (7) propionitrile, and (8) acetonitrile.

$$f - f' = (\epsilon - 1)/(2\epsilon + 1) - (n^2 - 1)/(2n^2 + 1) \quad (1)$$

The solvatochromic shift of the fluorescence (ν_{flu}) maxima of the LE and ICT bands can be expressed by the following equation[26−32]

$$\nu_{flu} = (-1/4\pi\epsilon_0)\cdot(2/hca^3)\cdot\mu_e^{ex}(\mu_e^{ex} - \mu_g)(f - f') + \text{const}' = m(\text{flu})(f - f') + \text{const}' \quad (2)$$

where, a is the equivalent spherical radius of the solute (Onsager radius) and ϵ, ϵ_0, and n are the dielectric constant, the vacuum permittivity, and the refractive index of the solvent, respectively. The variable μ_g is the ground-state dipole moment, and μ_e^{ex} refers to the dipole moment of the LE or ICT state.

The Onsager radius a (5.1 Å), was determined from Avogadro's number, assuming that the molecular density of **2** is equal to 1.0.[30] For the ground state dipole moment of **2** a value of $\mu_g = 6.0$ D was calculated on the basis of the crystal structure.[33,34] From the slope m(flu) for the ICT fluorescence obtained from Figure 4, μ_e^{ICT} was calculated to be 14D. Similarly, from the slope for the LE fluorescence in Figure 4, the dipole moment of the LE state (μ_e^{LE}) was estimated as 8D.

Effect of Temperature on Fluorescence Spectra. The effect of temperature on the fluorescence spectra of **2** and **4** in acetonitrile is shown in Figure 5. For **2** (Figure 5A), an increase in temperature results in a relative increase in intensity of the LE band, which is accompanied by a decrease in the intensity of the ICT band around 625 nm. This temperature dependence is attributed to the low-lying ICT undergoing a thermal back reaction to the LE state with increasing temperature (see Scheme 1). The change in enthalpy associated with this reaction will also depend on temperature, as the solvent polarity decreases with increasing temperature, which will affect the ICT/LE fluorescence quantum yield ratio. Observations similar to those described here for **2** were made for the temperature as well as solvent dependence of the fluorescence of **1** and **3**.

In most dual fluorescent compounds containing an amino group, this phenomenon has been attributed to conformational changes of the amino substituent.[13−18] Comparison of the fluorescence properties of **4** and **5** helps to determine the role of the amino group in the dual emission of the D/A-substituted butadienes discussed here. Compound **4** contains a dimethylamino group on the phenyl ring in addition to the pyrrolidino substituent, the latter being absent in **5**. The solvent effect on the emission spectrum of **4** indicates qualitative similarities with those of **1**−**3**. The LE band is more prominent in nonpolar solvents, whereas the ICT band predominates in polar solvents. The fluorescence maxima of **4** in various solvents are listed in Table 1. Significant differences can however be observed on comparing the effect of temperature on the fluorescence of **4** with that found for **1**−**3**. Figure 5B shows that, with increasing temperature, the overall fluorescence intensity of **4** in the LE and ICT spectral region increases unlike what was observed for **2** (Figure 5A).

Addition of trifluoroacetic acid (TFA) has an interesting effect on the shape and temperature dependence of the fluorescence spectrum of **4** (Figure 5C). The response of the fluorescence spectrum of **4** to temperature in the presence of TFA becomes similar to that for **2** (Figure 5A). With increasing temperature, there is a decrease in the intensity of the ICT band and an enhancement in the intensity of the LE band. This indicates that addition of TFA leads to protonation of the aromatic dimethylamino group of **4**. With the lone pair of the aromatic amino blocked by protonation and unable to partake in the ICT process, the compound behaves very much like the derivatives **1**−**3**, which do not have a dimethylamino group on the phenyl ring. The dual fluorescence observed in these compounds **1**−**4** can therefore be attributed to the presence of the amino group directly connected to the butadiene chain. The role of this amino group in the dual fluorescence of **1**−**4** was further confirmed by studying the fluorescence properties of **5**. For this compound, an increase in solvent polarity results in a bathochromic shift in the fluorescence spectrum (Table 1). An increase in temperature results only in a decrease in the fluorescence intensity (Figure 6). There was no evidence of dual luminescence. This again confirms that the amino group directly connected to the butadiene chain is the donor moiety responsible for the dual fluorescence in **1**−**4**.

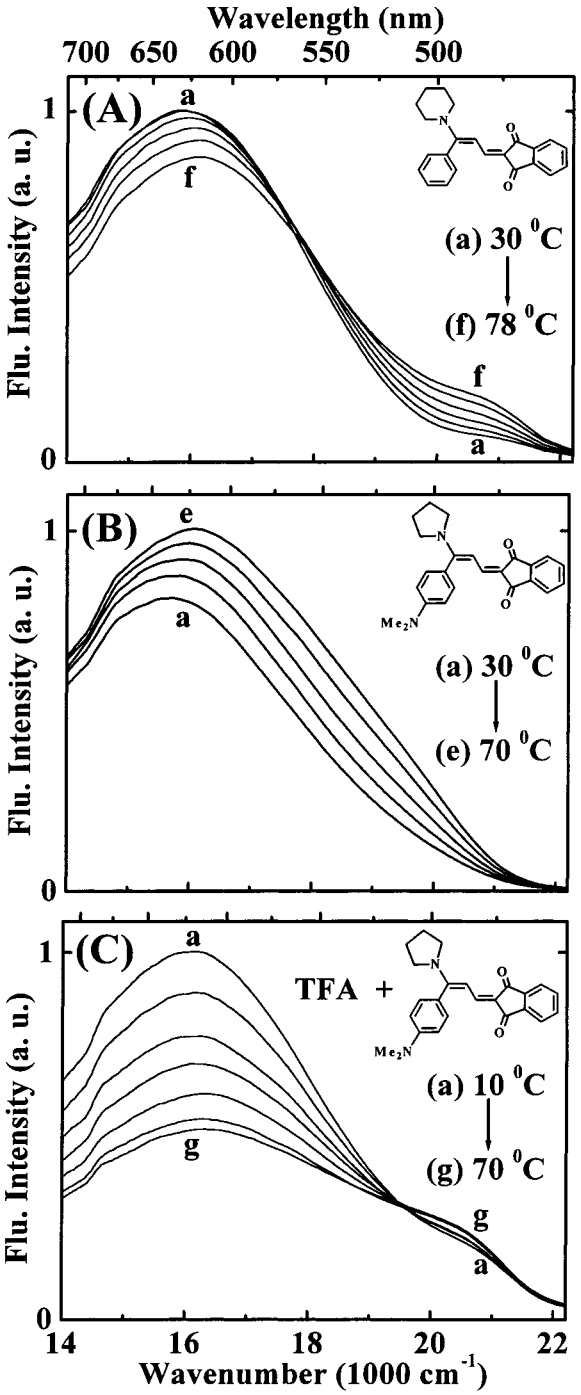

Figure 5. Temperature dependence of the fluorescence spectra of (A) **2** in acetonitrile, (B) **4** in acetonitrile and (C) **4** in acetonitrile containing 43 mM of trifluoroacetic acid. Temperature increase in steps of 10 °C.

Figure 7 shows a Stevens−Ban plot, ln(I'(ICT)/I(LE)) versus the reciprocal absolute temperature, for **1** in *n*-propylcyanide, where I'(ICT) is the intensity of the ICT emission band corrected for the increase in the bandwidth with increasing temperature, and I(LE) is the intensity of the LE band. The plot shows the pattern normally observed in the high-temperature limit (HTL) of a reversible ICT reaction described in Scheme 1, for which $k_d \gg 1/\tau'_0$.[35] The data points in Figure 7 were fitted to eq 3 by

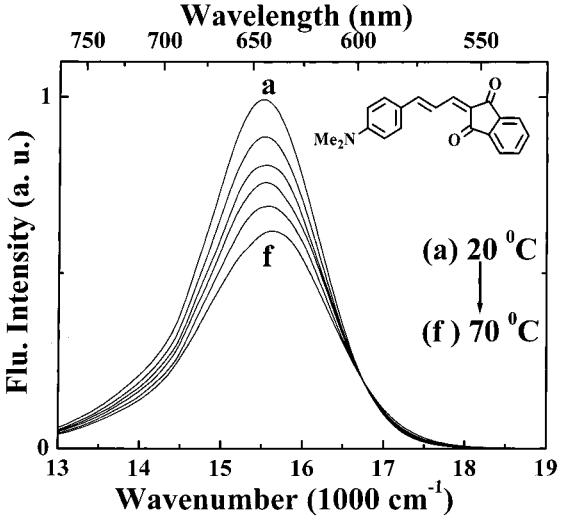

Figure 6. Temperature dependence of the fluorescence spectra of **5** in acetonitrile. Temperature increase in steps of 10 °C.

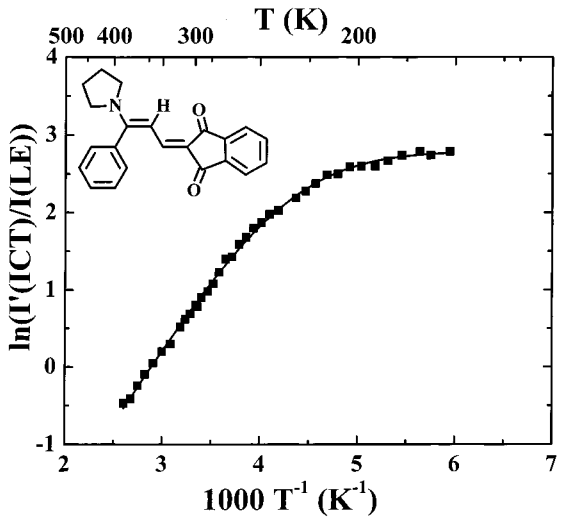

Figure 7. Stevens−Ban plot of the natural logarithm of the LE/ICT fluorescence intensity ratio I'(ICT)/I(LE), determined at the maxima of the ICT and LE emission bands, versus the reciprocal absolute temperature, for **1** in *n*-propylcyanide. The data points are fitted by a curve described by eq 3.

the nonlinear least-squares method. In eq 3 Φ'(ICT)/Φ(LE) represents the ICT to LE fluorescence quantum yield ratio.

$$\Phi'(\mathrm{ICT})/\Phi(\mathrm{LE}) \cong I'(\mathrm{ICT})/I(\mathrm{LE}) = k'_f[\mathrm{ICT}]/k_f[\mathrm{LE}] = k'_f/k_f \cdot k_a/(k_d + 1/\tau'_0) \quad (3)$$

The good fit of the data points to eq 3 supports our interpretation that dual emission in **1**−**4** originates from a reversible ICT reaction as represented by Scheme 1. The fit suggests a value approaching zero (0.2 ± 0.4 kJ/mol) for the activation energy, E_a of the forward ICT rate constant k_a.

Fluorescence Lifetimes. The picosecond fluorescence decay of compound **1** was measured at −40°C in three alkylcyanides of different polarity, acetonitrile (MeCN), propionitrile (EtCN), and butyronitrile (PrCN). The measurements were carried out at two wavelengths, one corresponding to the LE emission (480 nm) and the other at the maximum of the ICT fluorescence (650 nm), see Figure 8 and eqs 4 and 5. The fluorescence response function obtained at the maximum of the ICT emission band of **1** in the three alkylcyanides (Table 2) can be fitted with two exponentials (eq 5). A growing-in with a decay time τ_2 between

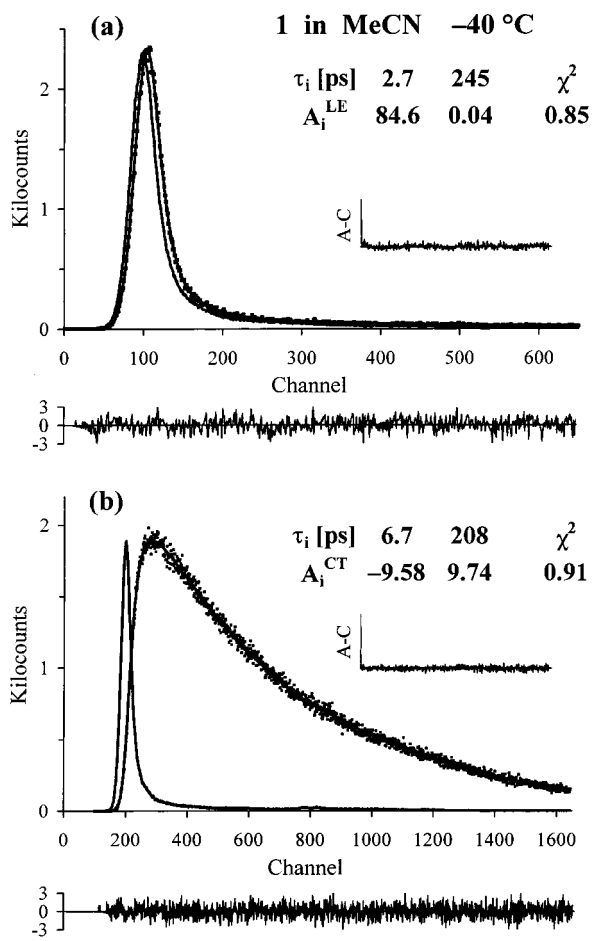

Figure 8. LE (a) and ICT (b) fluorescence response functions of **1** in acetonitrile at −40 °C. The decay times (τ_1, τ_2) and their preexponential factors A_{1i}^{LE} and A_{2i}^{ICT} are given in eqs 4 and 5. The shortest decay time τ_2 is listed first. The weighted deviations expressed in σ (expected deviations), the autocorrelation functions A−C, and the values for χ^2 are also shown. Excitation wavelength: 413 nm.

TABLE 2: Fluorescence Decay Times τ_1 and τ_2 and Their Amplitude Ratios (Eqs 4 and 5) Measured at the ICT (650 nm) and LE (480 nm) Fluorescence Bands of 1 in Three Solvents at −40 °C

solvent[a]	τ_2(ICT) [ps]	τ_1(ICT) [ps]	$-A_{22}/A_{21}$	τ_2(LE) [ps]	τ_1(LE) [ps]	A_{12}/A_{11}
MeCN	6.7	208	0.97	2.7	245	2100
EtCN	6.1	307	1.01	2.8	276	1000
PrCN	6.0	355	1.03	3.2	306	500

[a] MeCN: acetonitrile; EtCN: propionitrile; PrCN: butyronitrile.

6 and 7 ps is observed, whereas the longer decay time τ_1 increases with decreasing solvent polarity: 208 ps (MeCN), 307 ps (EtCN), and 355 ps (PrCN), see Table 2. The amplitude ratio $-A_{22}/A_{21}$ equals unity, which shows that the ICT state cannot be reached by direct light absorption from S_0 (Scheme 1)[23]

$$i_f(\mathrm{LE}) = A_{11}\exp(-t/\tau_1) + A_{12}\exp(-t/\tau_2) \quad (4)$$

$$i_f(\mathrm{ICT}) = A_{21}\exp(-t/\tau_1) + A_{22}\exp(-t/\tau_2) \quad (5)$$

The LE fluorescence decays (eq 4), on the other hand, are practically single exponential in all three solvents, with a decay time τ_2 around 3 ps (at the limit of the time resolution of our SPC setup, see the Experimental section) and a longer decay time τ_1 similar to that of the ICT decays, but with a large amplitude ratio A_{12}/A_{11} between 2100 and 500 (Figure 8 and

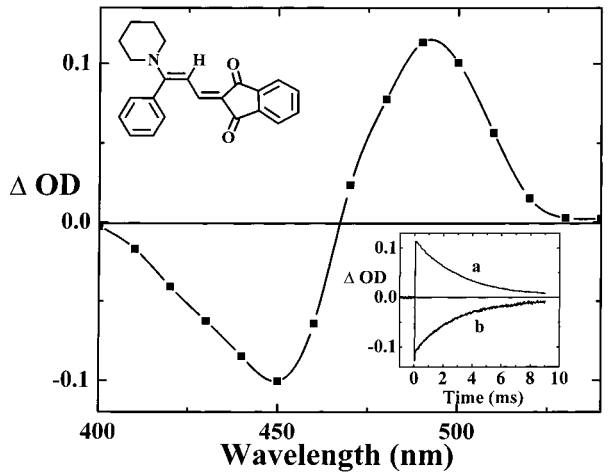

Figure 9. Transient absorption spectrum measured immediately following 355 nm laser pulse excitation of a solution of **2** in benzene. Inset shows the transient absorption profile at (a) 490 nm and (b) 450 nm.

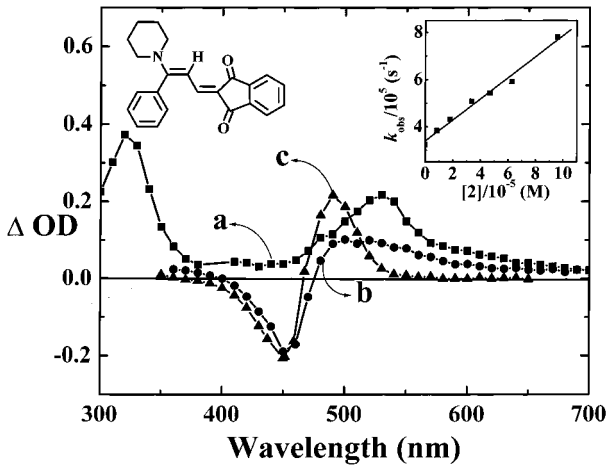

Figure 10. Transient absorption spectrum measured after 355 nm laser pulse excitation of argon-degassed solution of **2** and benzophenone in benzene: (a) 0.1 μs, (b) 5 μs, and (c) 10 μs. Inset shows the plot of the rate constant for decay of benzophenone triplet at 320 nm versus concentration of **2**.

SCHEME 2

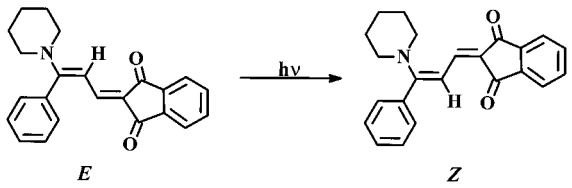

Table 2). Somewhat surprisingly, the LE and ICT decay times of **1** in PrCN are practically independent of temperature over the entire temperature range between −20 and −100 °C, measured at intervals of 20 °C. The same temperature independence was found for **1** in MeCN at 25 and −40 °C. With **2** in MeCN, similar decay times τ_1 were obtained for LE and ICT at these temperatures. Whereas the LE decay time τ_2 of ∼3 ps seems to be in accord with the relatively small ICT activation energy E_a of smaller than 1 kJ/mol (Table 2), the fact that the ICT rise-time τ_2 (6 to 7 ps) is different from the LE decay time is in conflict with the requirements of Scheme 1, which difference may be interpreted in terms of an additional intermediate species[36] or a time-dependent Stokes-shift. However, at the present stage of investigation, no direct evidence is available on the involvement of either of these two processes.

Photoisomerization. Direct excitation of **2** in benzene using a 355 nm laser pulse results in immediate formation of the transient absorption spectrum shown in Figure 9. Depletion is observed around 450 nm, which corresponds to the ground-state absorption maximum of **2**. A transient absorption maximum at 490 nm is also seen. The transient absorption at 490 nm decays back to the baseline by a first-order process, simultaneous with the recovery of the ground-state absorption of **2** around 450 nm (Inset, Figure 9). No change in the spectral shape of the transient absorption or in the rate of the transient decay was observed on using solutions bubbled with oxygen, which indicates that the observed changes cannot be due to formation of a long-lived triplet excited state of **2**. The fully reversible phototransformation observed on laser excitation may be attributed to isomerization of the butadiene moiety. The *trans* to *cis* photoisomerization of diphenylbutadienes has been extensively studied.[37−39] The most likely transformation in the present D/A-substituted butadienes is therefore the photoisomerization from the *E* to the *Z* isomer (*E*−*Z*), as shown in Scheme 2. It may be noted that isomerization around the double bond connected to the indanedione moiety would not lead to any change in the absorption spectrum due to the symmetry of this group.

The transient absorption spectrum (Figure 9) shows a shift of about 40 nm in the absorption maximum of the *Z* isomer compared to that of the *E* isomer. Similar bathochromic shifts on *E*−*Z* isomerization have been reported for several substituted olefins.[40−44]

Triplet Excited States. As discussed above, direct excitation of **2** does not lead to the formation of its triplet excited state. To study its triplet state properties, benzophenone was used as a triplet sensitizer. Figure 10 shows the transient absorption spectra measured on 355 nm laser pulse excitation of a solution of **2** in benzene, containing benzophenone. Under these conditions, the radiation is predominantly absorbed by benzophenone (94%). The transient absorption spectrum obtained immediately after the laser pulse (Figure 10, curve a) can be attributed to the triplet excited state of benzophenone, by comparison with the spectrum reported earlier.[45] The triplet of benzophenone is quenched by **2**, to yield the transient spectrum with a broad absorption in the region of 480−600 nm and a depletion around 450 nm (Figure 10, curve b). The rates of benzophenone triplet decay and growth of transient species are identical. From the dependence of observed rate constant for decay of the benzophenone triplet on the concentration of **2** (Inset, Figure 10), a rate constant, $k = 1.0 \times 10^{10}$ M^{-1} s^{-1}, is obtained indicating a diffusion-controlled process. Benzophenone is known to sensitize the triplet state of organic molecules. The transient absorption following the quenching process can therefore be attributed to the triplet state of **2**. The triplet excited state of **2** decays by a first-order process with a lifetime of 9 μs, to yield a fairly long-lived transient (Figure 10, curve c). The transient spectrum of this long-lived species is identical to the transient spectrum obtained on direct excitation of **2** (Figure 9). The decay of this species occurs by a first-order process with a lifetime of 3 ms, which is identical to the decay of the transient species formed on direct excitation of **2** (inset, Figure 9 and Table 3). These results indicate that the triplet excited state of **2** decays to the *Z* isomer of **2**. Oxygen bubbled solutions were studied in order to confirm that the $\mathbf{2}_Z$ isomer is mainly formed via the sensitized triplet excited state and not by direct excitation to

TABLE 3: Photoisomerization Data for the Butadiene Derivatives 1−5 at Room Temperature

			Benzene			Acetonitrile		
compd	λ_{max} (*E*)[a] (nm)	λ_{max} (*Z*)[b] (nm)	τ_T(μs)[c]	τ_z(ms)[d]	Φ_{E-Z}[e]	λ_{max} (*Z*)[b] (nm)	τ_z(μs)[d]	Φ_{E-Z}[e]
1	450	475	4	10	0.10	470	30	0.04
2	450	490	9	3	0.15	480	13	0.08
3	450	480	4	1.5	0.09	480	22	0.04
4	460	490	15	0.13	0.11	490	90	0.01
5	525	580	15	48 min*	0.09*	620*	8 min*	0.02*

[a] Absorption maximum of the *E* isomer. [b] Absorption maximum of the *Z* isomer. [c] Lifetime of the triplet excited state. [d] Lifetime of the *Z* isomer. [e] Quantum yield of *E*−*Z* photoisomerization measured by nanosecond laser flash photolysis. *Measured using steady-state photolysis.

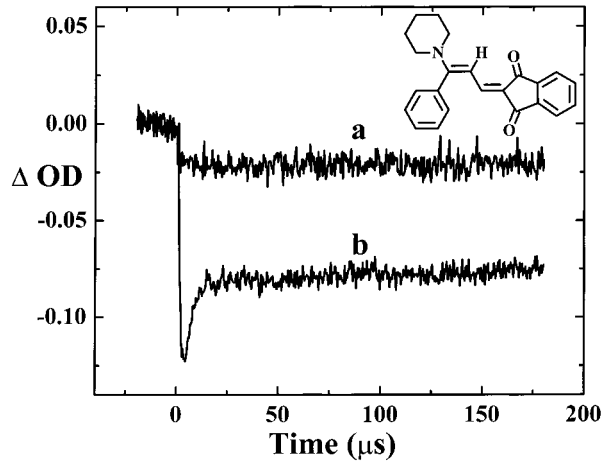

Figure 11. Transient absorption−time profiles recorded at 450 nm, following 355 nm laser pulse excitation of **2** (2×10^{-5} M) and benzophenone (3×10^{-3} M) in benzene. (a) oxygen bubbled and (b) argon purged.

SCHEME 3

$$BP \xrightarrow{h\nu} {}^3BP^*$$

$${}^3BP^* \longrightarrow BP$$

$${}^3BP^* + \mathbf{2}_E \longrightarrow {}^3\mathbf{2}^* + BP$$

$${}^3\mathbf{2}^* \xrightarrow{\tau = 9\ \mu s} \mathbf{2}_Z$$

$$\mathbf{2}_Z \xrightarrow{\tau = 3\ ms} \mathbf{2}_E$$

the singlet. In the presence of oxygen, the triplet state of benzophenone is quenched and only a small amount of the residual absorption, attributable to the *Z* isomer produced by direct excitation of **2**, was observed (Figure 11). This confirms that the major fraction of the *Z* isomer generated in the presence of benzophenone arises from the triplet state of **2**. The observed processes can be described by the mechanism shown in Scheme 3.

Quantum Yield of Photoisomerization. For estimating the photoisomerization quantum yield on direct excitation of **2**, the extinction coefficient of the *Z* isomer at 490 nm was first determined by the relative actinometry method using tris(2,2′-bipyridyl)ruthenium(II)chloride hexahydrate (Rubp) as actinometer.[46] Solutions of Rubp in water and of benzophenone and **2** in benzene (optically matched at 355 nm) were used. The extinction coefficient was estimated from the following relationship

$$\epsilon(\mathbf{2}_Z) = [\Delta OD_S\ \Phi_T(R)/\Delta OD_R\ Y(\mathbf{2}_Z)]\epsilon_R \qquad (6)$$

where $\epsilon(\mathbf{2}_Z)$ is the extinction coefficient of $\mathbf{2}_Z$ at 490 nm, ΔOD_S is the change in ΔOD at 490 nm for a solution of **2** containing benzophenone following the decay of the benzophenone triplet, ΔOD_R is the initial change in ΔOD at 370 nm for the Rubp solution, $\Phi_T(R)$ is the triplet quantum yield of Rubp, $Y(\mathbf{2}_Z)$ is the yield of $\mathbf{2}_Z$ and ϵ_R is the extinction coefficient of Rubp at 370 nm.

For estimating the extinction coefficient of the *Z* isomer of **2**, the following two assumptions were made: (1) the benzophenone quenched by **2** is quantitatively converted to the triplet state of **2**, and (2) the $^3\mathbf{2}^*$ thus formed is quantitatively converted to the $\mathbf{2}_Z$ isomer. On the basis of these assumptions, the yield $Y(\mathbf{2}_Z)$ of the $\mathbf{2}_Z$ isomer formed in the presence of varying concentration of **2** was calculated using the following equation (eq 7)

$$Y(\mathbf{2}_Z) = Y({}^3\mathbf{2}^*) = [(k^1_{obs} - k)/k^1_{obs}]\Phi_T({}^3BP^*) \qquad (7)$$

where k^1_{obs} is the observed rate constant for the decay of benzophenone in the presence of **2**, and k is the rate constant for decay of benzophenone in the absence of quencher, $Y(^3\mathbf{2}^*)$ is the triplet yield of **2** formed via energy transfer at different quencher concentrations, and $\Phi(^3BP^*)$ is the triplet quantum yield of benzophenone. Using $\Delta OD_S/Y(\mathbf{2}_Z) = 0.32$ obtained from the slope of a linear plot of ΔOD_S versus $Y(\mathbf{2}_Z)$ of solutions containing benzophenone and varying concentrations of **2**,[22] in eq 6, the extinction coefficient of the $\mathbf{2}_Z$ isomer was estimated as 1.3×10^5 M^{-1} cm^{-1} at 490 nm. Because the amount of the $\mathbf{2}_Z$ isomer formed will be equal to the amount of $\mathbf{2}_E$ isomer depleted, the extinction coefficient of the stable $\mathbf{2}_E$ isomer at 450 nm can be calculated by using eq 8 and assuming minimum overlap of the absorption bands of the two isomers

$$\epsilon(\mathbf{2}_E)\,/\,\epsilon(\mathbf{2}_Z) = \Delta OD(\lambda_{max}E)/\Delta OD(\lambda_{max}Z) \qquad (8)$$

This results in an $\epsilon(\mathbf{2}_E)$ value of 1.3×10^5 M^{-1} cm^{-1} at 450 nm, which closely matches the value of 1.1×10^5 M^{-1} cm^{-1} for $\epsilon(\mathbf{2}_E)$ at 450 nm obtained by using the conventional Beer−Lambert law. The close match in the extinction coefficient of the stable $\mathbf{2}_E$ isomer obtained using two very different methods justifies the assumptions mentioned above, made in estimating the extinction coefficient of the $\mathbf{2}_Z$ isomer. These results also indicate that a very small overlap exists between the absorption spectra of the *Z* and *E* isomers of **2**. Earlier reports on polyenes have shown that such isomers can have well-separated absorption bands with minimal overlap.[38−40]

Using the extinction coefficient of the $\mathbf{2}_Z$ isomer obtained above, the photoisomerization quantum yield ($\Phi(\mathbf{2}_Z)$) of **2** from the excited singlet state was estimated as 0.15 by the relative actinometry method, using Rubp as actinometer

$$\Phi(\mathbf{2}_Z) = [(\Delta OD_S\ \Phi_T(R))/(\Delta OD_R\ \epsilon(\mathbf{2}_Z))]\epsilon_R \qquad (9)$$

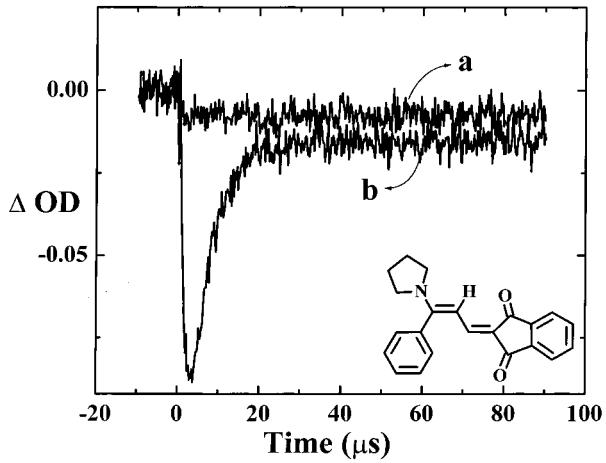

Figure 12. Transient absorption−time profiles recorded at 450 nm following 355 nm laser pulse excitation of **1** (2×10^{-5} M) and benzophenone (3×10^{-3} M) in benzene. (a) oxygen bubbled and (b) argon purged.

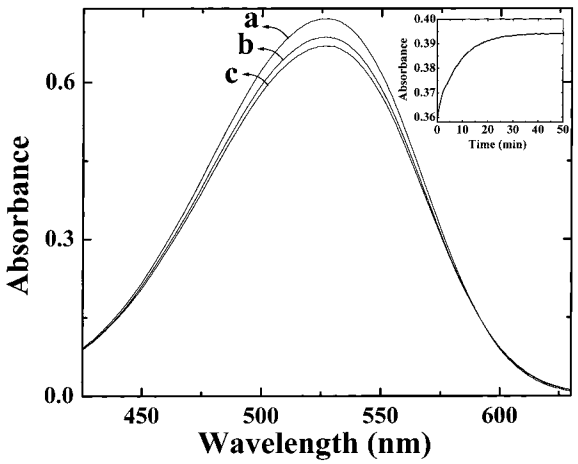

Figure 13. Effect of irradiation on the absorption spectrum of **5** in acetonitrile (a) before irradiation, (b) after 2 min, and (c) after 5 min; Inset shows recovery of the absorption at 520 nm following irradiation of **5** in acetonitrile for 3 min at 27 °C.

The results of the triplet-mediated photoisomerization of **3** were similar to that of **2**. For **1**, a different behavior was found. Although **1** undergoes photoisomerization from the singlet state in a manner similar to that of **2** and **3**, its triplet state properties are markedly different. Figure 12 shows the transient absorption profile at 450 nm on excitation of **1** in oxygen-saturated (curve a) and in argon-saturated (curve b) solutions containing benzophenone. In oxygen-saturated solutions, triplet energy transfer does not occur, and hence, the transient absorption observed is due to direct absorption by the substrate. From Figure 12, it becomes clear that the isomerization occurs mainly from the singlet state and that isomerization from the triplet state of **1** is very inefficient, unlike what is observed for **2** (Figure 11). To estimate the isomerization quantum yield of **1**, the extinction coefficient of its *Z* isomer was determined from the transient absorption spectrum, using eq 8, assuming a minimum overlap between the absorption bands of *E* and *Z* isomers. The results obtained for **2** justify this assumption for the D/A-butadiene derivatives studied here. The quantum yields of isomerization of **3** and **4** were estimated in a similar manner, assuming a minimum overlap between the absorption bands of the *E* and *Z* isomers, and the results are summarized in Table 3. The triplet excited-state properties of the D/A-substituted butadienes (**1**−**5**) are also summarized in Table 3. The photoisomerization quantum yields were lower in acetonitrile as compared to those in benzene.

The thermal *Z*−*E* isomerization of the D/A-substituted butadienes **1**−**4** occurs in the millisecond time domain in benzene. The lifetime of the *Z* isomers was much shorter in acetonitrile than in benzene. The rate constants for isomerization of D/A-substituted olefins are known to increase with increasing solvent polarity, due to reduction in bond order in such systems.[47]

Photoisomerization of 5. Laser pulse (532 nm) excitation of a solution of **5** in acetonitrile yields a weak transient absorption, which does not decay within 100 ms, indicating the formation of a long-lived species. Steady-state irradiation using a 520 nm band-pass filter resulted in a decrease in absorbance at 520 nm and a slight increase at 620 nm (Figure 13). This phototransformation is thermally reversible (inset, Figure 13).

For **5**, the all *trans* (*E*) isomer is expected to be the more stable form, based on comparison with similar compounds reported earlier.[48] Irradiation can lead to *E*−*Z* isomerization. The quantum yield of isomerization was estimated as 0.09 and 0.02 in benzene and acetonitrile, respectively, using Reinecke's salt actinometry as described in the Experimental Section. The thermal back reaction for **5**, measured by following the recovery of the absorption of the *E* isomer, occurred with lifetimes of 48 and 8 min in benzene and acetonitrile, respectively. This is much slower than that observed for the other butadienes **1**−**4** investigated here.

This difference may be attributed to efficient charge transfer from the amino nitrogen directly attached to the butadiene chain (**1**−**4**), which can reduce the bond order of the C═C double bond, thereby making the isomerization process faster. In **5**, which does not possess an amino group directly attached to the butadiene chain, the charge transfer from the aromatic amino nitrogen to the indanedione would be hindered by the energy barrier for the loss of aromaticity taking place on formation of the quinonoid structure. As the C═C double bond will be less affected in this case, it would result in slower *Z*−*E* isomerization of **5**.

Conclusion

Intramolecular charge transfer, triplet state properties, and photoisomerization were studied for the D/A-substituted butadienes **1**−**5**. Compounds **1**−**4**, which possess an amino substituent directly connected to the butadiene chain, show dual fluorescence from an LE state and a more polar ICT state. Compound **5**, which contains only an aromatic amino substituent connected to the butadiene chain, does not show dual fluorescence. The quantum yield of fluorescence is very low for these compounds, and the intersystem crossing efficiency is negligible. The compounds undergo *E*−*Z* photoisomerization from the excited singlet state with a quantum efficiency of about 0.10 in benzene. Internal conversion forms the main pathway for energy dissipation from the excited singlet state for this class of molecules. The triplet states of the butadienes were generated via energy transfer from the triplet state of benzophenone. The compounds containing diethylamino- (**3**) and piperidino- (**2**) substituents undergo *E*−*Z* isomerization quantitatively from the excited triplet state, whereas for the pyrrolidino-substituted derivatives, **1** and **4**, photoisomerization from the excited triplet state is inefficient. The rates for thermal *Z*−*E* isomerization of these derivatives are also highly sensitive to the nature of the amino substituent on the butadiene moiety (**2**∼**3**>**1**).

Acknowledgment. The authors would like to thank the Council of Scientific and Industrial Research, Government of India and the Volkswagen-Stiftung, Germany for supporting this work. We thank Dr. M. Noltemeyer, University of Göttingen, Germany for the X-ray analysis. This is Contribution No. RRLT-PRU-127 from RRL, Trivandrum.

Supporting Information Available: Full description regarding synthesis of the compounds studied and also supporting figures. This material is available free of charge via the Internet at http://pubs.acs.org.

References and Notes

(1) *Nonlinear Optical Properties of Organic Molecules and Crystals*; Vol. 1 and 2; Chemla, D. S., Zyss, J., Eds.; Academic Press: London, 1987.
(2) *Organic Materials for Nonlinear Optics*; Special Publication No. 69; Hann, R. A., Bloor, D., Eds.; Royal Society of Chemistry: Oxford, 1989.
(3) Burland, D. M.; Miller, R. D.; Walsh, C. A. *Chem. Rev.* **1994**, *94*, 31.
(4) Marder, S. R.; Perry, J. W. *Adv. Mater.* **1993**, *5*, 804.
(5) Paley, M. S.; Harris, M. J. *J. Org. Chem.* **1991**, *56*, 568.
(6) Stiegman, A. E.; Graham, E.; Perry, K. J.; Khundkar, L. R.; Cheng, L.-T.; Perry, J. W. *J. Am. Chem. Soc.* **1991**, *113*, 7658.
(7) Jen, A. K.-Y.; Rao, V. P.; Wang, K. Y.; Drost, K. J. *J. Chem. Soc., Chem. Commun.* **1993**, 90.
(8) Ching, K. C.; Lequan, M.; Lequan, R. M. *J. Chem. Soc., Faraday Trans.* **1991**, *87*, 2225.
(9) Coe, B. J. *Chem. Eur. J.* **1999**, *5*, 2464.
(10) Christopher, R. M.; Robert, J. T.; Lee, V. Y.; Swanson, S. A.; Betterton, K. M.; Miller, R. D. *J. Am. Chem. Soc.* **1993**, *115*, 12599.
(11) Das, S.; George, M.; Mathew, T.; Asokan, C. V. *J. Chem. Soc., Perkin Trans. 2* **1996**, *2*, 731.
(12) Singh, A. K.; Darshi, M.; Kanvah, S. *J. Phys. Chem. A* **2000**, *104*, 464.
(13) Zachariasse, K. A. *Chem. Phys. Lett.* **2000**, *320*, 8.
(14) Rettig, W.; Bliss, B.; Dirnbirger, K. *Chem. Phys. Lett.* **1999**, *305*, 8.
(15) Demeter, A.; Druzhinin, S.; George, M.; Haselbach, E.; Roulin, J.-L.; Zachariasse, K. A. *Chem. Phys. Lett.* **2000**, *323*, 351.
(16) Chudoba, C.; Kummrow, A.; Dreyer, J.; Strenger, J.; Nibbering, E. T. J.; Elsaesser, T.; Zachariasse, K. A. *Chem. Phys. Lett.* **1999**, *309*, 357.
(17) Il′ichev, Y. V.; Kühnle, W.; Zachariasse, K. A. *J. Phys. Chem.* **1998**, *102*, 5670.
(18) Rettig, W. In *Topics of Current Chemistry*, Vol. 169, Electron Transfer 1; Springer: Berlin, 1994; p 253.
(19) Takeuchi, S.; Tahara, T. *J. Phys. Chem. A* **1997**, *101*, 3052.
(20) Shimojima, A.; Tahara, T. *J. Phys. Chem. B* **2000**, *104*, 9288.
(21) Yamaguchi, S.; Hamaguchi, H.-O. *J. Chem. Phys.* **1998**, *109*, 1397.
(22) Details provided in the Supporting Information.
(23) Leinhos, U.; Kühnle, W.; Zachariasse, K. A. *J. Phys. Chem.* **1991**, *95*, 2013.
(24) Wegner, E. E.; Adamson, A. W. *J. Am. Chem. Soc.* **1966**, *88*, 394.
(25) Davis, R.; George, M.; Das, S.; Noltemeyer, M.; Zachariasse, K. A., unpublished results.
(26) Lippert, E.; Mall, F. *Z. Elektrochem.* **1954**, *58*, 718.
(27) Lippert, E. *Z. Elektrochem.* **1957**, *61*, 962.
(28) Lippert, E. *Z. Naturforsch.* **1955**, *10a*, 541.
(29) Kawski, A.; Gryczynski, I.; Jung, C.; Heckner, K.-H. *Z. Naturforsch.* **1977**, *32a*, 420.
(30) Il′ichev, Y. V.; Kühnle, W.; Zachariasse, K. A. *Chem. Phys. Lett.* **1996**, *211*, 441.
(31) Baumann, W.; Bischof, H.; Brittinger, J.-C.; Rettig, W.; Rotkiewicz, K. *J. Photochem. Photobiol. A: Chem.* **1992**, *64*, 49.
(32) Horng, M. L.; Gardecki, J. A.; Papazyan, A.; Maroncelli, M. *J. Phys. Chem.* **1995**, *99*, 17311.
(33) Schmidt, M. W.; Baldridge, K. K.; Boatz, J. A.; Elbert, S. T.; Gordon, M. S.; Jensen, J. J.; Koseki, S.; Matsunaga, N.; Nguyen, K. A.; Su, S.; Windus, T. L.; Dupuis, M.; Montgomery, J. A. *J. Comput. Chem.* **1993**, *14*, 1347.
(34) Gajewski, J. J.; Gilbert, K. E.; McKelvey, L. *Advances in Molecular Modelling*, Vol. 2; Liotta, D. Ed.; JAI Press: Greenwich, CT, 1990.
(35) Zachariasse, K. A. *Trends Photochem. Photobiol.* **1994**, *3*, 211.
(36) Lewis, F. D.; Weigel, W. *J. Phys. Chem. A:* **2000**, *104*, 8146.
(37) Görner, H. *J. Photochem.* **1982**, *19*, 343.
(38) Kawski, A.; Kuklinski, B.; Kubicki, A. *Z. Naturforsch.* **1993**, *48a*, 1177.
(39) Kawski, A.; Gryczynski, Z.; Gryczynski, I.; Wiczk, W.; Malak, H. *Z. Naturforsch.* **1991**, *46a*, 621.
(40) Lewis, F. D.; Yoon, B. A.; Arai, T.; Iwasaki, T.; Tokumaru, K. *J. Am. Chem. Soc.* **1995**, *117*, 3029.
(41) Lewis, F. D.; Yoon, B. A. *J. Photochem. Photobiol. A: Chem.* **1995**, *87*, 193.
(42) Arai, T.; Moriyama, M.; Tokumaru, K. *J. Am. Chem. Soc.* **1994**, *116*, 3171.
(43) Arai, T.; Iwasaki, T.; Tokumaru, K. *Chem. Lett.* **1993**, 691.
(44) Lewis, F. D.; Yang, J. S. *J. Phys. Chem.* **1996**, *100*, 14 560.
(45) Hoshino, H.; Shizuka, H. In *Photoinduced Electron Transfer*, Part C.; Fox, M. A., Chanon, M., Eds.; Elsevier: New York, 1988.
(46) Carmichael, I.; Hug, G. L. *J. Phys. Chem. Ref. Data* **1986**, *15*, 1.
(47) Schanze, K. S.; Mattox, T. F.; Whitten, D. G. *J. Am. Chem. Soc.* **1982**, *104*, 1733.
(48) Orlandi, G.; Zerbetto, F.; Zgierski, M. Z. *Chem. Rev.* **1991**, *91*, 867.